

NATIONAL ADVISORY COMMITTEE FOR AERONAUTICS

TECHNICAL NOTE 3027

INFLUENCE OF ROTOR-ENGINE TORSIONAL OSCILLATION

ON CONTROL OF GAS-TURBINE ENGINE GEARED

TO HELICOPTER ROTOR

By John C. Sanders

Lewis Flight Propulsion Laboratory
Cleveland, Ohio

NASA FILE COPY

NACA TN 3027

Loan expires on last date stamped on back cover.

PLEASE RETURN TO

REPORT DISTRIBUTION SECTION

LANGLEY RESEARCH CERTE

NATIONAL AERONAUTIOS
- SPACE ADMINISTRATE

FIRS DOCUMENT ON LOAN FROM THE FILES O

LANGLEY AFFORASTICAL LEBORATORY

Washington

October 1953

REQUESTS FOR PUBLICATIONS SHOULD BE ADDRESSED AS FOLIOWS:

NATIONAL ADVISORY COMMITTEE FOR AERONAUTICS 1704 - STRLET, N.W.

TECHNICAL NOTE 3027

INFLUENCE OF ROTOR-ENGINE TORSIONAL OSCILLATION ON CONTROL

OF GAS-TURBINE ENGINE GEARED TO HELICOPTER ROTOR

By John C. Sanders

SUMMARY

Equations were developed for the torsional motion of a gas-turbine engine geared to a helicopter rotor in which the rotor blades were hinged to the rotor shaft. The rotor system was simplified to yield simple third-order equations that can be used in the analysis of engine control. Comparison of the system response calculated from these equations with the experimentally observed frequency response of a rotor from a 2500-pound helicopter showed satisfactory agreement.

Calculations showed that the torsional motion arising from the hinged construction of the blades contributed to the instability of the engine-speed and engine-torque controls. Trends in stability and response of controls with increasing weight of helicopters were investigated.

INTRODUCTION

Investigation of the control of the speed of a gas turbine geared to a propeller is shown in reference 1 to involve the problem of controlling the speed of a single rotating body with damping forces from the engine and the propeller. When the propeller is replaced by a helicopter rotor, however, torsional flexibility between the gas turbine and the helicopter rotor may be sufficient to establish torsional oscillations. In this case, the torsional oscillation may contribute an unstabilizing influence to the engine control.

The torsional flexibility in the helicopter rotor arises from two sources: First, the long and highly stressed drive shaft permits considerable twisting; and second, in many rotors the blades are fastened to the hub by lag hinges, which, as shown in figure 1, permit the blades to swing relative to the hub in the plane of rotation. Centrifugal force tends to hold the blades in a radial position, while aerodynamic drag forces tend to make the blades fall behind a radial position.

The torsional oscillations of a rotor from a small helicopter (2500 lb gross wt) were measured and are reported in reference 2. The data revealed a badly underdamped resonance at 7.9 radians per second, which is a low enough frequency to influence the action of the engine control.

The investigation reported herein was conducted at the NACA Lewis laboratory to determine whether the torsional oscillations in helicopter rotors have a detrimental effect on the control of gas-turbine engines to which they are geared. The investigation was made by first establishing differential equations of motion of the rotor and then verifying the equations by comparing the calculated results with the observed oscillations reported in reference 2.

The effects of helicopter size and rotor weight on rotor dynamics were investigated, and the control characteristics of a gas-turbine engine in a large helicopter were studied. The control systems considered were speed and torque control by fuel flow.

SYMBOLS

The following symbols are used in this report:

a	radius from center of rotor shaft to drag hinge, ft
Ъ	distance from drag hinge to center of gravity of rotor blade, ft
С	coefficient of characteristic equation
С	dimension in geometry of force vectors, ft
c.g.	center of gravity
D	coefficient in characteristic equation
đ	dimension in geometry of force vectors, ft
E	coefficient of characteristic equation
е	dimension in geometry of force vectors, ft
F_{D}	drag force, 1b
F_{r}	centrifugal force, lb
Ft	tensile force, lb

f	radius at which Ft acts, ft
G	coefficient of characteristic equation
hp	horsepower of engine
I _e	inertia of engine rotor and gearing at rotor shaft speed, $$\operatorname{lb-ft}\sec^2$$
I_r	polar moment of inertia of rotor blades about center of rotor shaft, lb-ft \sec^2
$K_{\mathbb{C}}$	gain of control amplifier, (lb/sec)/(radians/sec)
K_{L}	loop gain of control
ka	effective spring constant of torque restoring rotor blades to radial positions, ft-lb/radian
kb	torsional spring rate of rotor shaft, ft-lb/radian
k_{D}	viscous-drag coefficient of dampers, (ft-lb)(sec)/radian
ke	rate of change of engine torque with engine speed at constant fuel flow, (ft-lb)(sec)/radian
k _r	rate of change of aerodynamic torque on rotor with change in rotor blade speed, (ft-lb)(sec)/radian
k _s	effective spring rate between engine and rotor blades, ft-lb/radian
$k_{\overline{W}}$	rate of change of engine torque with fuel flow, ft-lb/(lb fuel/sec)
kβ	rate of change of aerodynamic torque with change in rotor pitch at constant rotor blade speed, ft-lb/radian
L	lift or gross weight of helicopter, lb
M	mass of rotor blades, $(lb)(sec^2)/ft$
Ne	amplitude of engine speed variation, radians/sec
\overline{N}_{e}	engine speed, radians/sec
Nr	amplitude of rotor speed variation measured at centers of gravity of rotor blades, radians/sec

$\overline{\mathtt{N}}_\mathtt{r}$	rotor angular velocity measured at centers of gravity of rotor blades, radians/sec
$\left(\frac{\partial \overline{\mathbb{M}}_{\mathrm{e}}}{\partial \overline{\mathbb{M}}}\right)_{\mathrm{SS}}$	slope of steady-state, speed - fuel-flow characteristic
р	symbol for d/dt
\mathtt{Q}_{D}	amplitude of torque force developed by damper, ft-lb
Q_e	amplitude of engine-torque variation, ft-lb
$\mathtt{Q}_{\mathtt{r}}$	amplitude of rotor-torque variation, ft-lb
$Q_{\mathbf{S}}$	amplitude of shaft-torque variation, ft-lb
r _t	radius to tip of rotor, ft
W	amplitude of fuel-flow variation, lb/sec
α	amplitude of angular twist of rotor shaft, radians
β	amplitude of rotor-pitch variation, radians
ζ	amplitude of angular motion of rotor blades relative to center of rotor shaft, radians
ζ _{SN}	change in steady-state value of drag angle at constant rotor speed following change in rotor pitch, radians
θ	amplitude of angular deflection between engine and helicopter rotor blades, radians
$\tau_{_{\text{\tiny C}}}$	time constant of fuel system, sec
$ au_{ ext{d}}$	time constant of derivative action of control, sec
$ au_{ ext{e}}$	engine time constant, sec
$ au_{\dot{ extsf{l}}}$	time constant of integrator action of control, sec
$ au_{ ext{r}}$	rotor-blade time constant, $I_r/-k_r$, sec
ω	frequency of sinusoidal disturbance in rotor pitch, radians/sec

wn undamped natural frequency of engine-rotor system, radians/sec

 ω_r torsional pendulum frequency of rotor, $\sqrt{\frac{-k_s}{I_r}}$, radians/sec

EQUATIONS OF MOTION FOR ROTOR

In this section of the report, a simplified model of the rotorengine system is developed and the linear differential equations of motion are established. The important transfer functions are presented and examined.

Simplified Model of Rotor

A model of the rotor was used to obtain equations simple enough to be easily represented by an electronic analog. More complete statements of rotor-blade motion during forward flight, including the flexibility of the rotor-bearing mounts, appear in standard texts, such as reference 3. They are too complex for use in control study but could, perhaps, be simplified.

The articulated rotor system of figure 1 was considered to consist of two coaxial bodies in pure rotation, coupled by a torsional spring on the axis. This model is illustrated in figure 2. The engine-rotor inertia is represented as $I_{\rm e}$ and the inertia of the articulated blades about the rotor shaft is represented as $I_{\rm r}$. The spring has a stiffness composed of two terms: the torsional stiffness of the drive shaft and a stiffness corresponding to the centrifugal force that tends to restore the rotor blades to radial positions.

Consider first the balance of torques on the engine in figure 2:

$$Q_e + Q_s + Q_D = I_e dN_e/dt$$
 (1)

The aerodynamic torque Q_{e} delivered by the engine to the rotating system is

$$Q_{e} = k_{W}W + k_{e}N_{e}$$
 (2)

The torque Q_S of the equivalent spring is

$$Q_{s} = k_{s} \int (N_{e} - N_{r}) dt = k_{s} \theta$$
 (3)

where

$$k_{S} = Q_{S}/\theta \tag{4}$$

and

$$\theta = \int (N_e - N_r) dt$$
 (5)

The torque $Q_{\overline{D}}$ developed by the damper is

$$Q_{D} = -k_{D} (N_{e} - N_{r}) = -k_{D} d\theta/dt$$
 (6)

Substituting the values of Q_e , Q_s , and Q_D into equation (1) gives

$$I_e dN_e/dt = k_W W + k_e N_e + k_S \theta - k_D d\theta/dt$$
 (7)

The torque equation for the rotor is similarly derived. The aero-dynamic torque on the rotor is

$$Q_r = k_\beta \beta + k_r N_r \tag{8}$$

The rotor-torque equation becomes

$$I_r dN_r/dt = k_\beta \beta + k_r N_r - k_s \theta + k_D d\theta/dt$$
 (9)

Equations (7) and (9) can be reduced to a convenient dimensionless form by dividing by $I_r\omega_r^2$. The resultant equation can be expressed in terms of time constants τ_e and τ_r . Equation (7) becomes

$$\frac{N_{e}}{\omega_{r}} \frac{p}{\omega_{r}} = \frac{I_{r} k_{W}}{I_{e} (-k_{r})} \frac{1}{\tau_{r} \omega_{r}} \frac{W}{\omega_{r}} - \frac{\tau_{r}}{\tau_{e}} \frac{1}{\tau_{r} \omega_{r}} \frac{N_{e}}{\omega_{r}} - \frac{I_{r}}{I_{e}} \theta - \frac{I_{r}}{I_{e}} \frac{k_{D}}{(-k_{r})} \frac{1}{\tau_{r} \omega_{r}} \theta \frac{p}{\omega_{r}}$$

$$(10)$$

and equation (9) becomes

$$\frac{N_r}{\omega_r} \frac{p}{\omega_r} = \frac{k_\beta}{-k_r} \frac{1}{\tau_r \omega_r} \frac{\beta}{\omega_r} - \frac{1}{\tau_r \omega_r} \frac{N_r}{\omega_r} + \theta + \frac{k_D}{(-k_r)} \frac{1}{\tau_r \omega_r} \theta \frac{p}{\omega_r}$$
(11)

The reduction of equations (7) and (9) to dimensionless form has reduced the number of coefficients to be investigated. In equations (7) and (9), the coefficients are

$$I_e$$
, k_W , k_e , k_s , k_D , k_β , k_r , I_r

$$\frac{I_r}{I_e}$$
, $\frac{1}{\tau_r \omega_r}$, $\frac{\tau_r}{\tau_e}$, $\frac{k_D}{k_r}$, $\frac{k_{\beta}}{k_r}$, $\frac{k_W}{k_r}$

Thus, the number of coefficients have been reduced to six. The effects of only the first three are explored in this paper.

Equations (5), (7), and (9) define the motion of the engine-rotor system as functions of fuel-flow disturbances W and rotor-pitch disturbance β . The coefficient k_W is the slope of the torque - fuel-flow characteristic of the engine at constant speed. Similarly, k_e is the slope of the engine-torque - speed characteristic at constant fuel flow, k_{β} is the slope of the rotor-torque - pitch characteristic at constant speed, and k_r is the slope of the rotor-torque - speed characteristic at constant pitch. The system of equations (5), (7), and (9) therefore constitutes a linearization of the motion of the engine and rotor. Such a linearized representation is applicable to small excursions from a steady-state condition and is useful for study of control stability.

The system of equations (5), (7), and (9) or equations (5), (10), and (11) can be simulated directly by electronic analog and therefore represents the extent to which the equations need be developed. Solution of these equations to give transfer functions among the inputs and outputs will, however, yield useful information, because certain properties of the motion can be revealed by inspection of the equations.

Transfer Functions

The equations (5), (7), and (9) can be solved to yield an equation showing the response of N_r to W. If the derivative symbol d/dt is represented as p, this equation appears as follows:

$$N_{r} = \frac{pk_{D} - k_{s}}{p^{3}C + p^{2}D + pE + G} k_{W}W$$
 (12)

when C, D, E, and G are constants having the following values:

$$C = I_{e} I_{r}$$

$$D = -I_{e}k_{r} - I_{r}k_{e} + I_{e}k_{D} + I_{r}k_{D}$$

$$E = -I_{r}k_{s} + k_{e}k_{s} - I_{e}k_{s} - k_{e}k_{D} - k_{r}k_{D}$$

$$G = k_{s}k_{e} + k_{s}k_{r}$$
(13)

The remaining five transfer functions have the same denominator, but different numerators. These transfer functions are:

$$N_{r} = \frac{p^{2}I_{e} + p(k_{D} - k_{e}) - k_{s}}{p^{3}C + p^{2}D + pE + G} k_{\beta}$$
 (14)

$$N_{e} = \frac{p^{2}I_{r} + p(k_{D} - k_{r}) - k_{s}}{p^{3}C_{r} + p^{2}D_{r} + pE_{r} + G_{r}} k_{W}W$$
 (15)

$$N_{e} = \frac{pk_{D} - k_{s}}{p^{3}C + p^{2}D + pE + G} k_{\beta}\beta$$
 (16)

$$\theta = \frac{pI_r - k_r}{p^3C + p^2D + pE + G} k_W W$$
 (17)

$$\theta = \frac{-pI_e + k_e}{p^3C + p^2D + pE + G} k_{\beta} \beta$$
 (18)

Inspection of the denominator will, among other things, reveal the undamped natural frequency ω_n and the pendulum frequency ω_r of the rotor. If the energy dissipating coefficients $k_e,\,k_r,$ and k_D equal zero, the denominator becomes:

$$p^{3}(I_{e}I_{r}) + p^{2}(0) - p(I_{r}k_{s} + I_{e}k_{s}) + 0$$
 (19)

Equating this term to zero gives the characteristic equation:

$$p^{2}(I_{e}I_{r}) - (I_{e} + I_{r})k_{s} = 0$$
 (20)

The undamped natural frequency is

$$\omega_{\rm n} = \sqrt{\left(\frac{I_{\rm r}}{I_{\rm e}} + 1\right) \frac{k_{\rm s}}{I_{\rm r}}} \tag{21}$$

If the engine inertia $\, {\rm I}_{\rm e} \,$ is increased to infinity, the undamped natural frequency becomes the pendulum frequency of the rotor in torsion:

$$\omega_{\mathbf{r}} = \sqrt{\frac{k_{\mathrm{S}}}{I_{\mathrm{r}}}} \tag{22}$$

The steady-state gains between inputs and outputs are readily obtained from the transfer function by evaluating the transfer function at zero frequency; this is done by factoring the numerators and denominators so that their last terms are equal to unity. An important gain used in this report is the gain of engine speed to disturbance in fuel flow:

$$\left(\frac{\partial N_{\rm e}}{\partial W}\right)_{\rm SS} = \frac{k_{\rm W}}{-k_{\rm e} - k_{\rm r}} \tag{23}$$

This gain is needed in analysis of control systems involving speed and fuel flow.

SOLUTION OF EQUATIONS OF MOTION

Analog Representation

Solutions of the equations of motion were made with the help of an electronic analog. In this section, the analog representation used is presented, the manner of extending the representation to free-wheeling turbines is discussed, and the physical constants in the equation of motion are evaluated.

The analog representation chosen for investigation of control is a direct representation of the elementary equations (5), (7), and (9) rather than a construction of the transfer functions (12), (14), (15), (16), (17), and (18). The method chosen is the simpler of these two, because it requires only three integrators (equaling the number of energy-storage elements), and it requires that each physical constant be represented only once.

A direct representation of the equations of motion is shown in figure 3(a). In this figure, the transfer functions of the boxes are indicated. For example, the box containing $k_{\rm D}$ is an amplifier with a gain numerically equal to $k_{\rm D}$, and the block with $1/I_{\rm e}p$ is an integrator with an integrator time constant numerically equal to $I_{\rm e}$. It may be seen that the top row of boxes represents the equation of motion involving the engine speed $N_{\rm e}$; and the bottom row, the rotor speed $N_{\rm r}$. The subtracter and the box marked $k_{\rm S}/p$ represent equation (5), and the remaining box, marked $k_{\rm D}$, represents the damper.

The representation of a physical system in an electronic analog is usually made with all physical constants reduced to dimensionless form. Selection of scale factors is simplified, and the number of variables to be studied is reduced. In this study, the time scale was canceled

2977

by multiplying by the rotor pendulum frequency ω_r . The resulting analog representation, shown in figure 3(b), was used in studies subsequently presented in this report. In many applications, other reductions to dimensionless form may be preferable.

When the dimensionless representation is used in a control study, the loop gain of the control in terms of the dimensionless parameters is needed. The loop gain of the speed - fuel-flow control is constituted as follows:

$$K_{L} = \begin{bmatrix} \frac{1}{\tau_{r}\omega_{r}} \\ \frac{1}{\tau_{r}} \frac{\tau_{r}}{\tau_{e}} \frac{1}{\tau_{r}\omega_{r}} + \frac{1}{\tau_{r}\omega_{r}} \end{bmatrix} \begin{bmatrix} k_{W} \\ -k_{r} \end{bmatrix} K_{C}$$
(24)

In equation (24), the term $K_{\rm C}$, which is the gain of the control, has units of the ratio of fuel-flow change to speed change. Equation (24) is produced by reducing the engine gain (eq. (23)) to dimensionless form and multiplying by $K_{\rm C}$.

In analyzing a control system, the second term on the right side of equation (24) is usually represented by an amplifier. The first term is already represented in figure 3(b).

Extension to Free-Wheeling Turbine Drives

The analysis and the analog representation are easily extended to the case of the free-wheeling turbine drive. In this system, a gasturbine engine provides hot gas at high pressure to an independent drive turbine that is geared to the rotor shaft. The operating conditions of the gas-turbine engine are approximately independent of the load applied to the drive turbine.

The analog representation of the rotor and its free-wheeling drive turbine is made by a simple replacement of the fuel-flow input by the two new inputs, gas pressure and temperature to the drive turbine. The analog representation of the response of gas pressure and temperature to fuel flow supplied to the gas turbine is taken from figure 4(b) of reference 4.

Evaluation of Physical Constants

Torsional coefficient k_s . - Coefficients in equations (5), (7), and $\overline{(9)}$ that pose difficulties in evaluation are k_s and k_r . In

particular, the torsional elasticity $k_{\rm S}$ is important, because the adequacy of the assumption of pure rotation depends upon the accuracy with which $k_{\rm S}$ can be chosen.

The total torsional deflection amplitude of the center of gravity of a blade, relative to the engine rotor, is θ . This deflection is composed as follows:

$$\theta = \zeta + \alpha \tag{25}$$

where ζ is the amplitude of angular motion of the blades and α is the amplitude of twist of the drive shaft. Now

$$\zeta = Q_{S}/k_{a} \tag{26}$$

$$\alpha = Q_{S}/k_{D} \tag{27}$$

therefore,

$$\theta = Q_{S} \left(\frac{1}{k_{a}} + \frac{1}{k_{b}} \right) \tag{28}$$

In figure 2, ks was defined by the relation

$$k_{S} = \frac{Q_{S}}{\theta} \tag{29}$$

Combining equations (28) and (29) and eliminating $Q_{\rm S}/\theta$ yield

$$k_{S} = \frac{1}{\frac{1}{k_{a}} + \frac{1}{k_{b}}}$$
 (30)

The torsional elasticity \mathbf{k}_b of the shaft is easily determined; evaluation of the rotor deflection constant \mathbf{k}_a remains to be accomplished.

The geometry of the force vectors acting on a rotor blade is shown in figure 4. The rotor blade is hinged to the hub at a distance a from the center of the drive shaft. In steady rotation, the centrifugal force F_r acting through the center of gravity of the blade attempts to hold the blade so that its center of gravity is on a line with the hinge and the center of the rotor shaft. An aerodynamic drag force F_D normal to the radius causes the blade to swing back to an angle ζ where the tensile force F_t along the axis of the blade has a component parallel, equal, and opposite to the drag force.

The definition of $k_{\mathbf{a}}$ is

$$k_{a} = dQ_{s}/d\zeta \tag{31}$$

Now

$$Q_s = F_t f = \frac{b}{e} F_r f$$

 $F_r = M(d + e) \overline{N}_r^2$

and

$$f = a \sin \zeta$$

For small values of ζ ,

$$f = a \zeta$$

Hence

$$Q_s = M\overline{N}_r^2(d + e) \frac{b}{e} a$$

whence

$$\frac{dQ_s}{d\zeta} = k_a = \left(\frac{d + e}{a}\right) \left(\frac{b}{e}\right) a^2 M\overline{N}_r^2$$

A close approximation having more convenient dimensions is

$$k_{a} = \left(\frac{a + b}{a}\right) a^{2} M \overline{N}_{r}^{2}$$
 (32)

Damping coefficient k_r . - The rotor damping coefficient k_r is easily found if the shaft horsepower in steady state is known. The definition of k_r is

$$k_{r} = -\left(\frac{\partial Q}{\partial \overline{N}_{r}}\right)_{\beta} \tag{33}$$

where the subscript indicates that the rotor pitch β is held constant while the slope of the torque-speed curve is measured. If consideration is given to the fact that at constant rotor pitch the torque is proportional to the square of the rotor speed,

$$k_r = -2 \times 550 \frac{hp}{\overline{N}_r^2} \tag{34}$$

In the dimensionless representation of figure 3(b), the rotor time constant τ_r is used. The rotor time constant is

$$\tau_r = \frac{I_r}{-k_r} = \frac{I_r \overline{N}_r^2}{2 \times 550 \text{ hp}}$$
 (35)

COMPARISON OF CALCULATED AND EXPERIMENTALLY

OBSERVED TORSIONAL MOTION

A critical comparison of torsional motion calculated by use of equations (5), (7), (9), and (32) with experimental observation is necessary, because these equations are based upon approximations. Experimental data of the type needed for this comparison are contained in reference 2.

In reference 2, measurements of the torsional oscillatory response of a helicopter rotor to a sinusoidal disturbance in rotor pitch are reported. The tests were performed on a rotor from a 2500-pound helicopter. The rotor was mounted on a helicopter test tower and driven by a 1350-horsepower reciprocating engine. Pertinent details of the rotor dimensions and test equipment are given in table I. The data used for comparison in the present report are the data for no oil damping shown in figure 2 of reference 2.

Calculation of Rotor Motion

The analog representation of figure 3(b) was used in calculating the rotor motion. The following coefficients were determined using the data from table I:

Coefficient	Value		
ka	-22,800 (ft-lb)(sec)/radian		
ks	-15,000 ft-lb/radian		
kr	-263 (ft-lb)(sec)/radian		
$\omega_{\mathtt{r}}$	5.22 radians/sec		
τ_r	2.10 sec		
$1/(\tau_r\omega_r)$	0.0913		
I_r/I_e	1.34		
k_{D}	0 (ft-lb)(sec)/radian		

The engine damping term $\,k_{e}$ (or $\tau_{e})$ is not reported in reference 2; it therefore had to be estimated. This estimation was made by assuming the indicated horsepower at constant throttle setting to be independent of engine speed and the friction torque of the engine to be proportional to the square of the engine speed. In the test, the engine, which was operated at 55 percent of the speed for maximum power, delivered 9.6 percent of its maximum power. The friction power was computed for these conditions on the assumption that the friction was in the same proportion as that in the Plymouth engine shown in figure 311, page 49, of reference 5. The computation yielded the following results:

$$k_r = -756$$
 (ft-lb) sec/radian $\tau_e = 0.542$ sec

Hence,

$$\frac{I_e}{I_r} \frac{\tau_r}{\tau_e(\tau_r \omega_r)} = 0.26$$

Comparison with Experimental Observation

The calculated and the observed torsional motion of the rotor are compared in figure 5 where drag-angle amplification is shown as a function of the frequency of the sinusoidal disturbance in rotor pitch. The drag-angle amplification is defined as the ratio of the amplitude of drag-angle oscillation ζ at the selected disturbance frequency ω to the change in the steady-state value of the drag angle at constant rotor speed when a change in rotor pitch of the same magnitude as the amplitude of the sinusoidal disturbance in pitch is made. The rotor-pitch frequency ω is made dimensionless by dividing by $\overline{N}_{\rm r}^2$, which is constant at 23 radians per second. The circles indicate data points reported in reference 2, and the curve shows the response computed using the analog representation of figure 3(b).

The data are in excellent agreement with the computed response. The resonant frequency is in close agreement - 0.35 times the rotor speed. The damping, as indicated by the drag-angle amplification factor at resonance, shows much better agreement than can normally be expected in view of the uncertainties in estimating the damping terms.

A disagreement between calculated and observed response occurs at high frequency, above a dimensionless frequency of 0.42. The increasing divergence between calculated and observed response at higher frequencies is interpreted as an indication that a system of differential

equations of higher than the third order represented in equations (5), (7), and (9) is needed, because the rotor blades can oscillate about their own centers of gravity in addition to having their centers of gravity oscillate around the rotor shaft.

In general, the agreement between calculated and observed response indicates that the differential equations (5), (7), and (9) and the analog representations in figure 3 will give satisfactory results in the analysis of engine control. With very large helicopters (50,000 lb gross wt) having heavy rotor blades, the resonant frequency will be so low that the error above the resonant frequency may become serious. Further investigation of the representation of the frequency response above resonance and additional careful measurement of response in this frequency range are needed.

Other Responses of the Rotor of Reference 2

As a matter of interest, other responses of the rotor described in reference 2 were computed. The frequency responses of engine speed and rotor speed (blade centers of gravity) to sinusoidal changes in rotor pitch and the transient responses to a step change in rotor pitch were calculated on the electronic analog. These responses are presented in figure 6 in the form of photographs of an oscilloscope screen.

The frequency response to rotor pitch disturbance is shown in figure 6(a). The blade-angle input in figure 3(b) was excited by a sweep-frequency oscillator that produced a sine wave, the frequency of which increased linearly with time. The x-axis of the oscilloscope was so synchronized with the sweep-frequency generator that, in the photograph, the x-axis is proportional to frequency. The y-axis was attached to the proper output, thereby creating an oscilloscope image comparable with the frequency response in figure 5, with the exception that the scales are linear rather than logarithmic. The drag-angle response shown should be the same as previously presented in figure 5.

The frequency response of engine speed is interesting in that a pronounced minimum occurs between zero frequency and resonance. At this "antiresonance" frequency, disturbances in rotor pitch have practically no effect on engine speed.

The corresponding transient response to a step change in rotor pitch is shown in figure 6(b). The highly underdamped oscillatory motion superimposed upon the exponential drift toward equilibrium is obvious. The oscillations in torque have an amplitude almost equal to the total changes in torque produced.

CONTROL STABILITY

The stability of engine speed and torque controls was investigated using the analog of figure 3(b) as a representation of the engine. Before making this study, however, it was necessary to estimate the proper dynamic coefficients for a large rotor to match a gas-turbine engine for which the dynamic coefficients were known. In this section of the report, the effects of helicopter weight on rotor dynamics are first investigated, and a rotor to match a 2700-horsepower gas turbine is chosen. Then, the stability of engine-speed and torque controls are explored.

Effect of Helicopter Weight on Rotor Dynamics

The gas-turbine engine for which the dynamic coefficients are known produces 2700 horsepower. The rotor for which the dynamic properties are known (the rotor studied in ref. 2) should be used with a 210-horsepower engine. This rotor was tested with a 1350-horsepower reciprocating engine. If the power-weight ratio of the helicopter is assumed to be 0.085 horsepower per pound regardless of weight, the 2700-horsepower turbine would be suitable for a 32,000-pound helicopter.

The dimensions and properties of a rotor suitable for a 32,000-pound helicopter may be computed by use of the data presented in table II. In this table, two different laws of rotor weight are used: One law makes the blade weight proportional to the helicopter plan form area, whereas the other law makes the blade weight proportional to the three-halves power of the helicopter weight. The first law is probably closer to what may be accomplished, but the results are somewhat optimistic in that the weight of a large rotor would be underestimated.

The effect of helicopter gross weight on the rotor dynamic coefficients is shown in figure 7. This figure was computed using the dimensions of the rotor for the 2500-pound helicopter and assuming the law of direct proportionality in table II. The dimensions of a rotor for a 32,000-pound helicopter were estimated, and the characteristics of a gas-turbine engine having a time constant of 1 second and an inertia of 1.15 pound-foot second2 (applicable to 2700 hp engine) were assumed. The engine time constant and the ratio of the inertia of the engine to that of the rotor were then assumed to be independent of helicopter gross weight. The resonant frequency and drag angle and the frequency response of engine speed to fuel flow were determined with the aid of the electronic analog of figure 3(b). The results presented in figure 7 show that the drag-angle amplification, engine-speed amplification, and resonant frequency decrease with increasing gross weight of the helicopter. The significant parameters for a gross weight of 32,000 pounds are listed in the following table together with those applicable to the test equipment used in securing the data of figure 5:

Parameter	Helicopter gr	oss weight, lb
	32,000	2500
Radius of rotor, ft	68	19
Rotor speed, radians/sec	6.43	23.0
ω _r , radians/sec	1.46	5.22
Engine inertia at engine speed, lb-ft sec ²	1.15	
Engine speed, radians/sec	1497	
Engine inertia at rotor speed I_e , $lb-ft\ sec^2$	62,000	
I _r /I _e	1.45	1.34
$1/(\tau_{r}\omega_{r})$	0.324	0.0914
$I_e au_r$		
$\overline{I_r} \overline{\tau_e(\tau_r \omega_r)}$	0.462	0.26

Comparison of the properties of the large helicopter and the small helicopter cannot be made because the engine for the smaller helicopter was a reciprocating engine and that for the large helicopter, a turbine-propeller engine.

Control system. - The control systems studied are shown in figure 8. Figure 8(a) shows a proportional-plus-integral control of engine speed in which speed is controlled by manipulation of fuel flow. An integrator time constant τ_i of 1.45 seconds and a fuel-system lag τ_c of 0.2 second were used throughout the studies. The rotor system was simulated by the analog of figure 3(b). Except where otherwise noted, the properties of the 32,000 pound helicopter were used.

Effect of torsional motion on control response. - A direct impression of the effect of the torsional motion on control response and stability can be obtained by comparing the responses of an articulated rotor and the response of a rigid rotor system having the same inertia and power input. This comparison is made in figure 9. Figure 9(a) shows the transient response of the articulated rotor and figure 9(b), the response of the rigid rotor. Computations for the rigid rotor are given in the appendix. The control used in each case had a loop gain of 2.5.

The oscillatory contribution of the articulated rotor is evident in a comparison of figures 9(a) and 9(b). A much larger overshoot in torque occurs with the articulated rotor than with the rigid rotor, and the time to establish a new equilibrium is much longer with the former system.

As a matter of interest, the transient responses of the engine rotor systems with articulated and rigid rotors without engine controls are shown in figures 9(c) and 9(d). The articulated rotor exhibits an underdamped high-frequency oscillation superimposed upon an exponential response, whereas the rigid rotor exhibits only a smooth exponential response.

It is concluded that stable control of engine speed by fuel flow can be established, but that the control system will be more oscillatory than it would be if used on a perfectly rigid rotor system.

Selection of engine-speed control. - The control with the high loop gain, 2.5, needed for accurate speed control shows a 22 percent overshoot in torque. The overshoot is determined by scaling the torque in figure 9(a). This torque overshoot may be practically eliminated by reducing the gain, as shown in figure 10. In this case the loop gain was reduced to 0.9. The low loop gain is shown to have the disadvantage of permitting a large excursion in engine speed. The speed excursion at the low gain is two times the speed excursion at high gain.

Effect of gross weight on speed control. - The effects of helicopter gross weight on dynamic response as well as the dynamic coefficients are shown in figure 7. It may be seen that not only did the resonant frequency decrease with increasing gross weight (as would be expected), but also that the damping of the resonant oscillation increased, as revealed by the decreasing trend in the ratio of resonant amplification to steady-state amplification. This effect is a result of the assumption that the rotor-blade weight is proportional to blade plan form area.

The corresponding variation of control behavior with change in gross weight is shown in figure 11. The loop gain above which continuous oscillation occurs is shown to increase to a value of 3.7 at a gross weight of 20,000 pounds, and further increase in gross weight has no effect on this stability limit. This decrease in loop gain at the low gross weight is attributable to the comparatively low damping of the rotor. With the high gross weight, the loop gain is only 3.7; whereas, for a rigid rotor, the loop gain is 17. Thus, the torsional motion of the rotor contributes greatly to the instability of the engine control.

Effect of rotor blade weight on control. - As pointed out in the section on the Effect of Helicopter Weight on Rotor Dynamics, the method used to estimate rotor weight might give low estimated rotor weights for large helicopters. In a method that gives weights that are probably too high for large helicopters, the weight of the rotor is assumed to be proportional to the volume of the rotor blade and, hence, proportional to the three-halves power of the helicopter gross

weight. Formulas for the dynamic constants under this assumption are given in table II. Extrapolation of the inertia of the small rotor of reference 2 to a size adequate for a 32,000-pound helicopter results in an inertia $I_{\rm r}/I_{\rm e}$ of 51.8 as compared with 1.45 when the law of direct proportion is assumed.

The effect of the inertia ratio on the maximum stable loop gain of the engine-speed control is shown in figure 12; the dimensions of the rotor were held constant, and only the weight and inertia were varied. As the rotor weight is allowed to increase, the maximum permissible loop gain decreases. Analysis for inertia ratios above 11.6 was impossible with the particular analog equipment used.

Transient responses of a helicopter having a rotor four times the mass (inertia ratio of 5.8) of that used in figure 9 are shown in figure 13. Figure 13(a) shows that the torsional oscillation is much less damped than that of the lighter rotor; the speed responses are, of course, much slower than with the lighter rotor.

Torque control. - The torque control shown in figure 8(b) was investigated. This control had the same components and coefficients as the speed control except that it was found necessary to add derivative action to the calculator. The derivative time constant τ_d was adjusted to meet the stability requirements of the control.

The torque control proved to be very prone to oscillate. Divergent oscillatory instability occurred above a loop gain of 2.9, and at lower loop gain the system showed oscillation.

A very smooth response was obtained at the high loop gain of 4.1 when a derivative time constant τ_d of 0.6 second was used. The system was very sensitive to both gain and derivative time constant and would break into continuous oscillation with either a higher or a lower derivative time constant.

Although a torque control could be effective, it would have a strong tendency to oscillate.

CONCLUSIONS

Analysis was made of the effect of the torsional oscillations in hinged rotor blades in a helicopter on the stability of engine controls on a gas-turbine engine geared to the rotor. The analysis led to the following conclusions:

2977

CM-3 bac

- l. Torsional oscillation of the articulated blades contribute considerably to the instability of engine controls. The unstabilizing action is more evident in torque control by fuel flow than in enginespeed control by fuel flow.
- 2. Increasing the mass of rotor blades reduces the stability of control systems, thereby necessitating lower loop gains and resulting in greater excursions in rotor speed.
- 3. The rotor-engine system may be represented adequately by two rotating masses connected by a torsional spring. The resonant frequency and damping were accurately represented, but the amplitude response above resonance was underestimated.

Lewis Flight Propulsion Laboratory
National Advisory Committee for Aeronautics
Cleveland, Ohio, August 12, 1953

APPENDIX - RESPONSE OF RIGID ROTOR

The response of a rigid rotor can be derived by setting the deflection θ in equations (5), (7), and (9) equal to zero and solving for N_e . The resultant equations are

$$N_e(I_e + I_r)p = k_\beta \beta + k_W W + (k_e + k_r)N_e$$
 (A1)

$$-Q_s = k_W W + k_e N_e - I_e N_e p$$
 (A2)

These equations, when reduced to the same dimensionless parameters used for the articulated rotor, become:

$$\frac{N_{e}}{\omega_{r}} \frac{p}{\omega_{r}} \left[\frac{I_{e}}{I_{r}} + 1 \right] = \frac{1}{\tau_{r} \omega_{r}} \frac{k_{W}}{(-k_{r})} \frac{W}{\omega_{r}} + \frac{1}{\tau_{r} \omega_{r}} \frac{k_{\beta}}{(-k_{r})} \frac{\beta}{\omega_{r}} - \frac{N_{e}}{\omega_{r}} \frac{1}{\tau_{r} \omega_{r}} \left[\frac{I_{e} \tau_{r}}{I_{r} \tau_{e}} + 1 \right]$$
(A3)

$$\frac{\left(\frac{Q_{s}}{I_{r}}\right)}{\omega_{r}^{2}} = \frac{kW}{(-k_{r})} \frac{1}{\tau_{r}\omega_{r}} \frac{W}{\omega_{r}} - \frac{I_{e}\tau_{r}}{I_{r}\tau_{e}} \frac{1}{\tau_{r}\omega_{r}} \frac{N_{e}}{\omega_{r}} - \frac{I_{e}}{I_{r}} \frac{N_{e}}{\omega_{r}} \frac{p}{\omega_{r}}$$
(A4)

Analog representations of these equations are shown in figure 14. Figure 14(a) is a direct representation in real time and is a construction of equations (A1) and (A2). Figure 14(b) is a nondimensional representation and is a construction of equations (A3) and (A4).

For the 32,000-pound helicopter, the following coefficients were found:

$$\frac{I_{e}}{I_{r}} + 1 = 1.69$$

$$\left[\frac{I_{e}}{I_{r}} \frac{\tau_{r}}{\tau_{e}} + 1\right] = 0.795$$

$$\left[\frac{I_{e}\tau_{r}}{I_{r}\tau_{e}}\right] = 0.472$$

REFERENCES

- 1. Himmel, Seymour C., and Krebs, Richard P.: The Effect of Changes in Altitude on the Controlled Behavior of a Gas-Turbine Engine. Jour. Aero. Sci., vol. 18, no. 7, July 1951, pp. 433-441.
- 2. Carpenter, Paul J., and Peitzer, Herbert E.: Response of a Helicopter Rotor to Oscillatory Pitch and Throttle Movements. NACA TN 1888, 1949.
- 3. Young, Raymond A.: Helicopter Engineering. The Ronald Press Co. (N.Y.), 1949.
- 4. Ketchum, J. R., and Craig, R. T.: Simulation of Linearized Dynamics of Gas-Turbine Engines. NACA TN 2826, 1952.
- 5. Lichty, Lester C.: Internal Combustion Engines. Fifth ed., McGraw-Hill Book Co., Inc., 1939.

TABLE I. - DIMENSIONS AND PROPERTIES OF HELICOPTER ROTOR AND

ENGINE USED IN TEST

Data from ref. 2.]

Engine speed at test conditions, rpm	Helicopter rotor:			
Blade moments of inertia about their centers of gravity (3 blades), lb-ft sec ² Blade center-of-gravity location from vertical pin axis, ft Vertical-pin-axis location from center of rotation, ft Drive-shaft torsional stiffness, ft-lb/radian Effective moment of inertia of engine and gearing referenced to rotor shaft speed, lb-ft sec ² Rotor shaft speed, radians/sec Shaft horsepower Engine: Rated horsepower Rated engine speed, rpm Engine speed at test conditions, rpm	Blade radius, ft			7.0
(3 blades), lb-ft sec ² Blade center-of-gravity location from vertical pin axis, ft . 5.76 Vertical-pin-axis location from center of rotation, ft . 0.757 Drive-shaft torsional stiffness, ft-lb/radian . 43,800 Effective moment of inertia of engine and gearing referenced to rotor shaft speed, lb-ft sec ² . 410 Rotor shaft speed, radians/sec	Blade Weight, 3 blades, including drag hings areals	•	•	. 19
Vertical-pin-axis location from center of rotation, ft	Diago moments of there a about their contact			
Vertical-pin-axis location from center of rotation, ft	Plade court Sec			. 224
Drive-shaft torsional stiffness, ft-lb/radian 43,800 Effective moment of inertia of engine and gearing referenced to rotor shaft speed, lb-ft sec ² Rotor shaft speed, radians/sec 23 Shaft horsepower 25 Rated horsepower 350 Engine: Rated engine speed, rpm 2400 Engine speed at test conditions, rpm 3700	find the state of	-		F 70
Effective moment of inertia of engine and gearing referenced to rotor shaft speed, lb-ft sec ² Rotor shaft speed, radians/sec Shaft horsepower Engine: Rated horsepower Rated engine speed, rpm Engine speed at test conditions, rpm 43,800 43,800 410 42,800 410 42,800 410 42,800 410 42,800 410 42,800 410 42,800 410 410 42,800 410 410 42,800 410 410 410 410 410 410 410 410 410 4	vertical pin-axis location from center of rotation et			0 555
enced to rotor shaft speed, lb-ft sec ²	Dilve-Bildie Corsional Stiffness ft-lh/redien	•	•	17 000
Shaft horsepower	TITCOULVE MOMETLY OF INETTING OF engine and gooming modern			
Shaft horsepower	Potential to rotor shaft speed, lb-ft sec2			. 410
Engine: Rated horsepower Rated engine speed, rpm Engine speed at test conditions, rpm	ricool shale speed, radians/sec			07
Rated horsepower	Shart horsepower	•	•	126
Engine speed at test conditions, rpm	Engine:	•	•	. 146
Engine speed at test conditions, rpm	Rated horsenower			
ingline speed at test conditions, rpm	Rated engine great			1350
ingline speed at test conditions, rpm	Fracing areas speed, rpm			2400
Helicopter gross weight, lb 2500	inglie speed at test conditions, rpm			1320
	nelicopter gross weight, lb			2500

TABLE II. - EFFECT OF HELICOPTER GROSS WEIGHT ON ROTOR DIMENSIONS AND PROPERTIES

Coefficient	Proportional	Three-halves
	(a)	(b)
Horsepower	cľ	L
Ir	L^2	L5/2
r _{t.}	L1/2	L1/2
k _a	L	$L^{3/2}$
k _s	T,	L3/2
	1/L ^{1/2}	$1/L^{1/2}$
$\omega_{\rm r}$	T 2	1,2
k _r	Constant	L1/2
τ_{r}	T.2	T.2
I _e	1	1
$\tau_{\rm e}$	Constant	Constant
Ir/Ie	Constant	L ^{3/2}
$1/(\tau_r\omega_r)$	L ^{1/2}	Constant
$I_{\rm e}$ $ au_{ m r}$	1.1/2	7 /7
$\overline{I_r} \overline{\tau_e(\tau_r \omega_r)}$	П	l/L
τ_e/τ_r	Constant	1/L ^{1/2}

^aRotor weight assumed proportional to plan form area.

^bRotor weight assumed proportional to threehalves power of blade plan form area.

^CGross weight of helicopter.

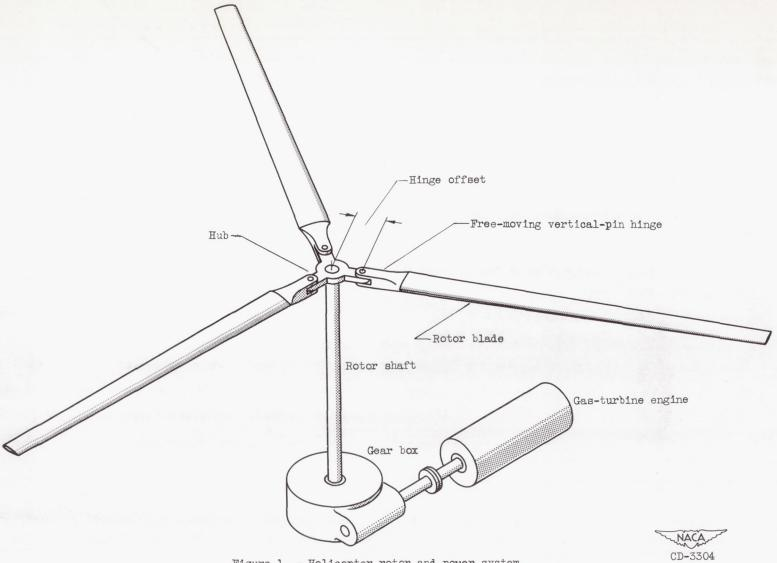
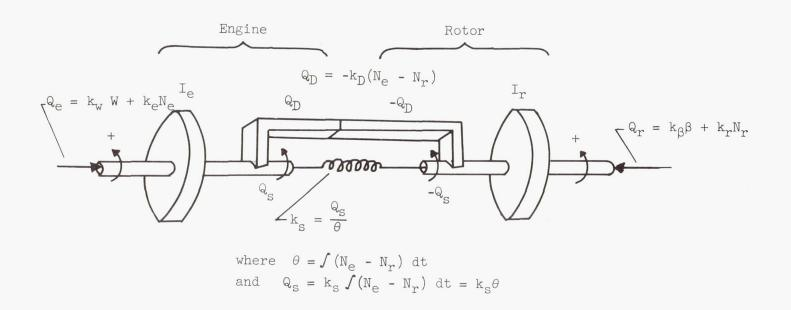
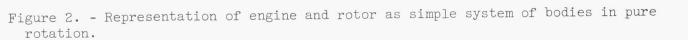
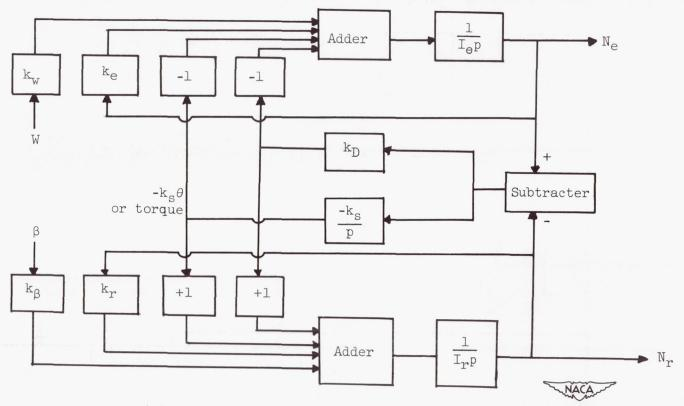


Figure 1. - Helicopter rotor and power system.







(a) Direct representation of system in real time.

Figure 3. - Analog representation of articulated helicopter rotor and engine.

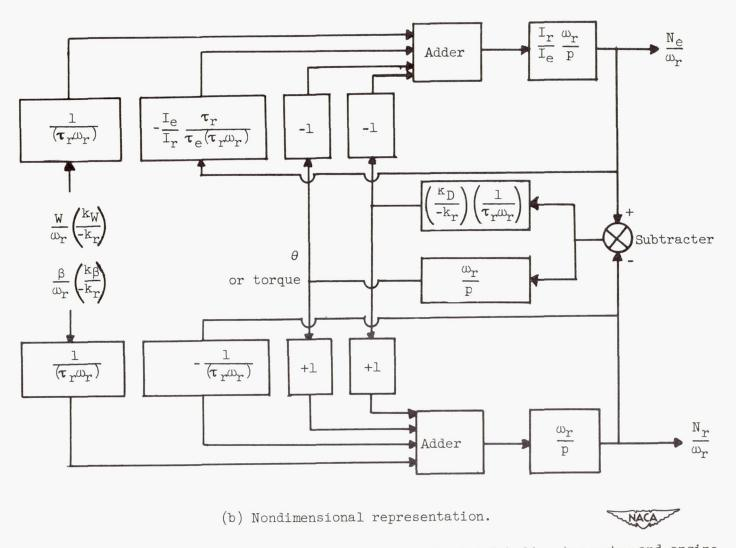


Figure 3. - Concluded. Analog representation of articulated helicopter rotor and engine.

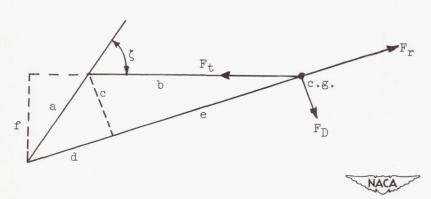


Figure 4. - Geometry of force vectors acting on rotor.

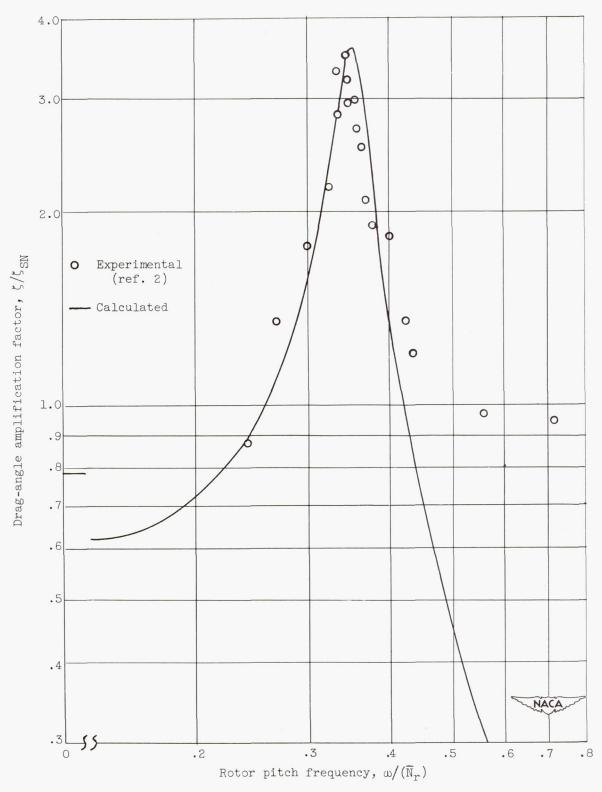
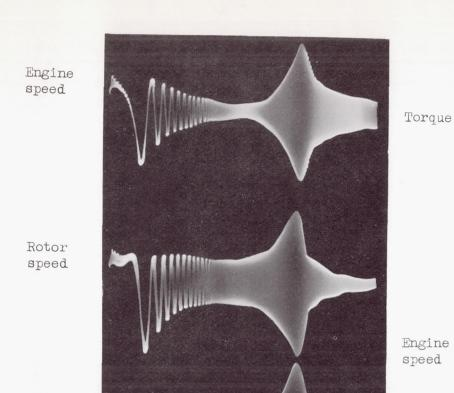
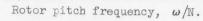


Figure 5. - Frequency response of blade drag angle to disturbance in rotorpitch angle.



C-33325

Drag angle or torque



(a) Frequency response to disturbance in rotor pitch.

(b) Transient response to step disturbance in rotor pitch.

Time, sec.

7.7

0

Figure 6. - Example of results obtained with analog representation of rotor-engine system presented in figure 2. ω

Rotor speed

.568

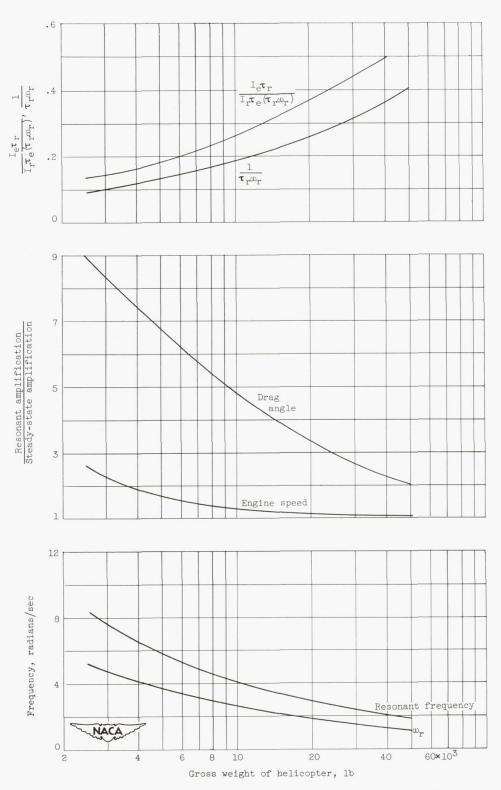
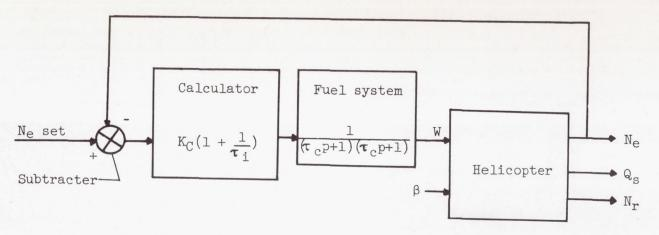
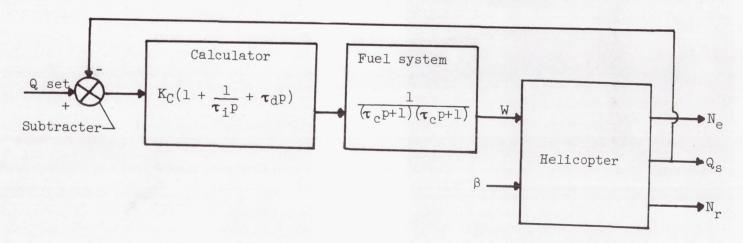


Figure 7. - Effect of helicopter weight on dynamic characteristics of rotor.



(a) Engine-speed control by fuel flow.



(b) Engine-torque control by fuel flow.



Figure 8. - Control systems investigated ($\tau_{\rm i}$, 1.45 sec; $\tau_{\rm c}$, 0.2 sec).

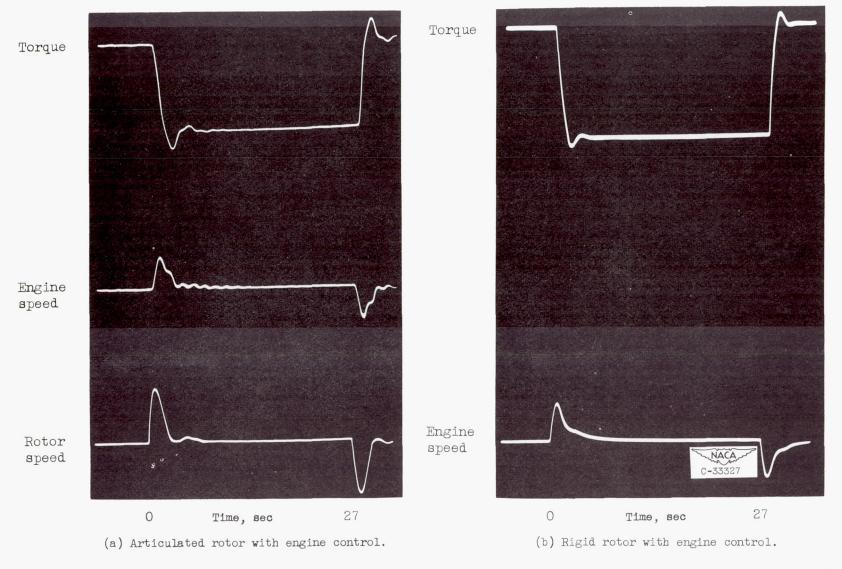


Figure 9. - Comparison of transient responses of an articulated and a rigid helicopter rotor to step change in rotor pitch. Helicopter weight, 32,000 pounds; control-loop gain, 2.5.

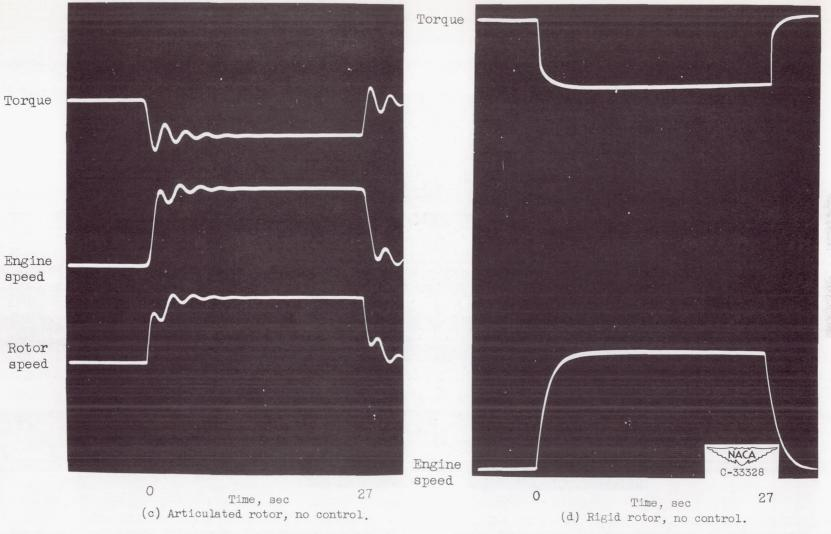
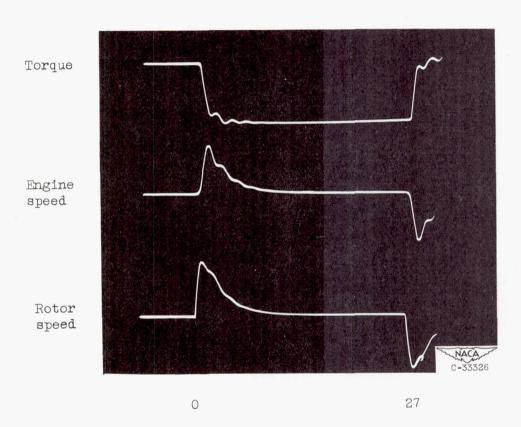


Figure 9. - Concluded. Comparison of transient responses of an articulated and a rigid helicopter rotor to step change in rotor pitch. Helicopter weight, 32,000 pounds; control-loop gain, 2.5.



Time, sec

Figure 10. - Transient response of articulated rotor system with control-loop gain adjusted to highest giving no significant overshoot in torque. Response to step change in rotor pitch; control-loop gain, 0.9.

Figure 11. - Effect of helicopter gross weight on stability of engine-speed controlled by fuel flow.

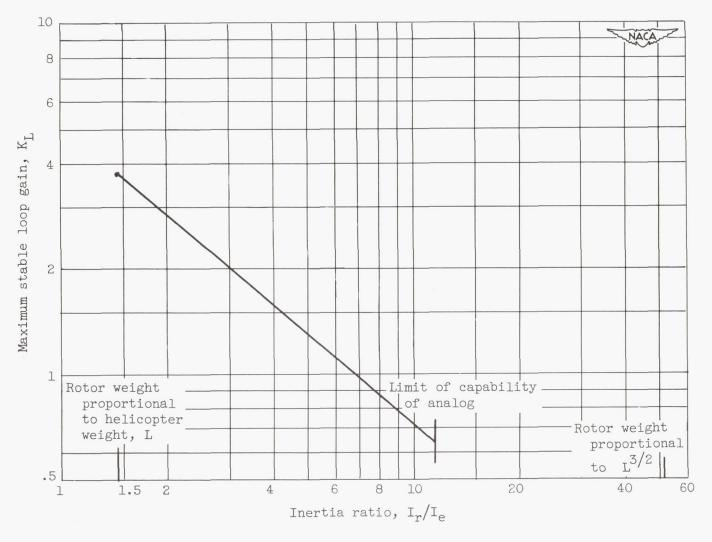


Figure 12. - Effect of rotor weight (inertia) on stability limit of engine-speed control in helicopter weighing 32,000 pounds. Control, integral plus proportional; integrator time constant, 1.45; control lag, 0.2 second.

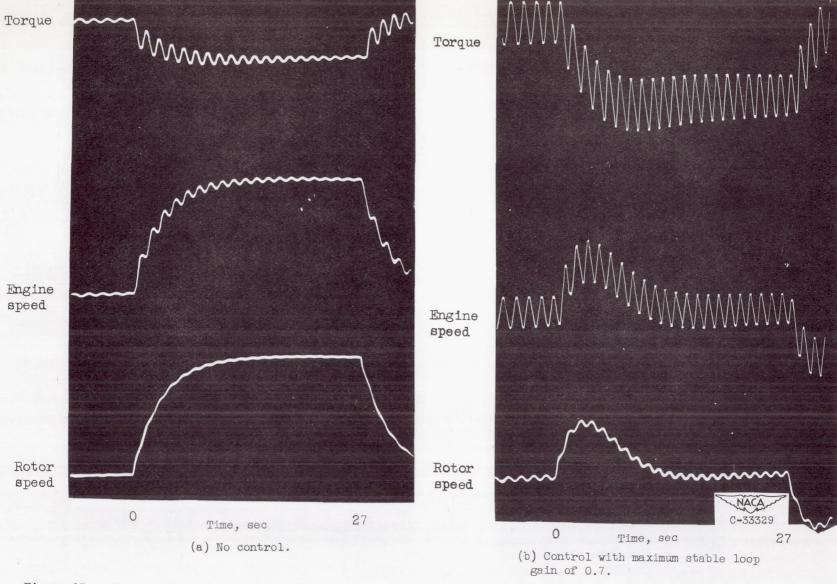
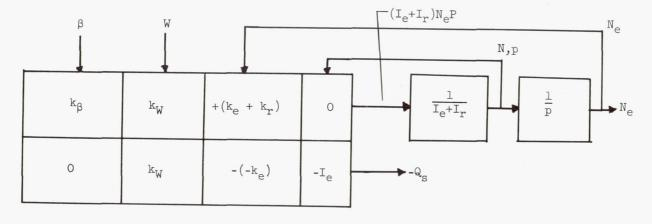
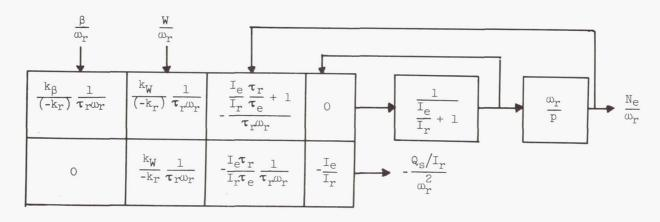


Figure 13. - Transient responses of 32,00-pound helicopter having rotor with four times weight represented in figure 9. Inertia ratio, 11.6.



(a) Direct representation in real time.



(b) Nondimensional representation.



Figure 14. - Analog representation of rigid helicopter rotor and engine.

NACA-Langley - 10-27-53 - 1000

LL62 ·